

# J|A|C|S

## A R T I C L E S

Published on Web 00/00/0000

### Detailed Structural Investigation of the Grafting of [Ta(=CH*t*Bu)(CH<sub>2</sub>*t*Bu)<sub>3</sub>] and [Cp\*TaMe<sub>4</sub>] on Silica Partially Dehydroxylated at 700 °C and the Activity of the Grafted Complexes toward Alkane Metathesis

Erwan Le Roux,<sup>†,‡</sup> Mathieu Chabanas,<sup>†,‡</sup> Anne Baudouin,<sup>†</sup> Aimery de Mallmann,<sup>†</sup>  
Christophe Copéret,<sup>\*,†</sup> E. Alessandra Quadrelli,<sup>†</sup> Jean Thivolle-Cazat,<sup>†</sup>  
Jean-Marie Basset,<sup>\*,†</sup> Wayne Lukens,<sup>§</sup> Anne Lesage,<sup>||</sup> Lyndon Emsley,<sup>\*,||</sup> and  
Glenn J. Sunley<sup>⊥</sup>

*Contribution from the Laboratoire de Chimie Organométallique de Surface (UMR 9986  
CNRS/ESCPE Lyon), ESCPE Lyon, F-308-43 Boulevard du 11 Novembre 1918,  
F-69616 Villeurbanne Cedex, France, Chemical Sciences Division, Lawrence Berkeley National  
Laboratory, Berkeley, California 94720, Laboratoire de Chimie (UMR 5532 CNRS/ENS),  
Laboratoire de Recherche, Conventionné du CEA (23V), Ecole Normale Supérieure de Lyon,  
46 Allée d'Italie, F-69364 Lyon Cedex 07, France, and BP Chemicals Ltd., Hull Research and  
Technology Center, Saltend, Hull, HU128DS, U.K.*

Received June 14, 2004; E-mail: basset@cpe.fr; coperet@cpe.fr; lyndon.emsley@ens-lyon.fr

**Abstract:** The reaction of [Ta(=CH*t*Bu)(CH<sub>2</sub>*t*Bu)<sub>3</sub>] or [Cp\*Ta(CH<sub>3</sub>)<sub>4</sub>] with a silica partially dehydroxylated at 700 °C gives the corresponding monosiloxy surface complexes [(=SiO)Ta(=CH*t*Bu)(CH<sub>2</sub>*t*Bu)<sub>2</sub>] and [(=SiO)Ta(CH<sub>3</sub>)<sub>3</sub>Cp\*] by eliminating a σ-bonded ligand as the corresponding alkane (H–CH<sub>2</sub>*t*Bu or H–CH<sub>3</sub>). EXAFS data show that an adjacent siloxane bridge of the surface plays the role of an extra surface ligand, which most likely stabilizes these complexes as in [(=SiO)Ta(=CH*t*Bu)(CH<sub>2</sub>*t*Bu)<sub>2</sub>(=SiOSi=)] (**1a'**) and [(=SiO)Ta(CH<sub>3</sub>)<sub>3</sub>Cp\*(=SiOSi=)] (**2a'**). In the case of [(=SiO)Ta(=CH*t*Bu)(CH<sub>2</sub>*t*Bu)<sub>2</sub>(=SiOSi=)], the structure is further stabilized by an additional interaction: a C–H agostic bond as evidenced by the small *J* coupling constant for the carbenic C–H (*J*<sub>C–H</sub> = 80 Hz), which was measured by *J*-resolved 2D solid-state NMR spectroscopy. The product selectivity in propane metathesis in the presence of [(=SiO)Ta(=CH*t*Bu)(CH<sub>2</sub>*t*Bu)<sub>2</sub>(=SiOSi=)] (**1a'**) as a catalyst precursor and the inactivity of the surface complex [(=SiO)Ta(CH<sub>3</sub>)<sub>3</sub>Cp\*(=SiOSi=)] (**2a'**) show that the active site is required to be highly electrophilic and probably involves a metallacyclobutane intermediate.

## Introduction

The interaction of organometallic complexes with oxide surfaces such as silica or alumina has been studied for 30 years.<sup>1–5</sup> The first application of these materials was to the generation of highly active heterogeneous polymerization catalysts, followed by applications to other catalytic processes such as hydrogenation, olefin and alkane metathesis, Fischer Tropsch, or oxidation. This approach is referred to as surface organometallic chemistry (SOMC), and its main objective is the transfer of concepts and tools from molecular chemistry to surface science.<sup>6</sup> The recent development of advanced spectro-

scopic techniques has greatly helped to characterize the exact nature of active sites of these systems.<sup>7–10</sup> Notably, we show how it is almost essential to combine the use of several analytical techniques to avoid making misleading conclusions. In this light, we discuss our results in comparison to previous studies carried out on these systems.<sup>11</sup> In the following study, we study and compare the reactivity of silica partially dehydroxylated at 700 °C with two tantalum complexes, [Ta(=CH*t*Bu)(CH<sub>2</sub>*t*Bu)<sub>3</sub>] and [Cp\*TaMe<sub>4</sub>]. The structure of each surface complex and the role of the silica surface on these structures will be discussed, highlighting the advantage of a rigorous multistep approach to

<sup>†</sup> Laboratoire de Chimie Organométallique de Surface, ESCPE Lyon.

<sup>‡</sup> Taken in part from his Ph.D. thesis.

<sup>§</sup> Lawrence Berkeley Laboratory.

<sup>||</sup> Laboratoire de Chimie, ENS Lyon.

<sup>⊥</sup> BP Chemicals.

- (1) Ballard, D. G. H. *Adv. Catal.* **1973**, *23*, 263–325.
- (2) Yermakov, Y. I.; Kuznetsov, B. N.; Zakharov, V. A. *Stud. Surf. Sci. Catal.* **1981**, *8*, 522 pp.
- (3) Basset, J. M.; Choplin, A. *J. Mol. Catal.* **1983**, *21*, 95–108.
- (4) Evans, J. *NATO Adv. Study Inst. Ser., Ser. C* **1988**, *231*, 47–73.
- (5) Scott, S. L.; Basset, J. M.; Nicolai, G. P.; Santini, C. C.; Candy, J. P.; Lecuyer, C.; Quignard, F.; Choplin, A. *New J. Chem.* **1994**, *18*, 115–122.

- (6) Copéret, C.; Chabanas, M.; Petroff Saint-Arroman, R.; Basset, J.-M. *Angew. Chem., Int. Ed.* **2003**, *42*, 156–181.
- (7) Petroff Saint-Arroman, R.; Chabanas, M.; Baudouin, A.; Copéret, C.; Basset, J.-M.; Lesage, A.; Emsley, L. *J. Am. Chem. Soc.* **2001**, *123*, 3820–3821.
- (8) Chabanas, M.; Quadrelli, E. A.; Fenet, B.; Copéret, C.; Thivolle-Cazat, J.; Basset, J.-M.; Lesage, A.; Emsley, L. *Angew. Chem., Int. Ed.* **2001**, *40*, 4493–4496.
- (9) Lesage, A.; Emsley, L.; Chabanas, M.; Copéret, C.; Basset, J.-M. *Angew. Chem., Int. Ed.* **2002**, *41*, 4535–4538.
- (10) Chabanas, M.; Baudouin, A.; Copéret, C.; Basset, J.-M.; Lukens, W.; Lesage, A.; Hediger, S.; Emsley, L. *J. Am. Chem. Soc.* **2003**, *125*, 492–504.
- (11) Ahn, H.; Marks, T. J. *J. Am. Chem. Soc.* **2002**, *124*, 7103–7110.

**Table 1.** Solid-State NMR Data for Solid **1**

ligand	$\delta^1\text{H/ppm}$	$\delta^{13}\text{C/ppm}$	$J_{\text{C-H/Hz}}$
$=\text{CHCMe}_3$	4.2	247	80
$=\text{CHCMe}_3$		47	
$=\text{CHCMe}_3$	1.0	31	126
$-\text{CH}_2\text{CMe}_3$	1.0	95	125
$-\text{CH}_2\text{CMe}_3$		31	
$-\text{CH}_2\text{CMe}_3$	1.0	31	126

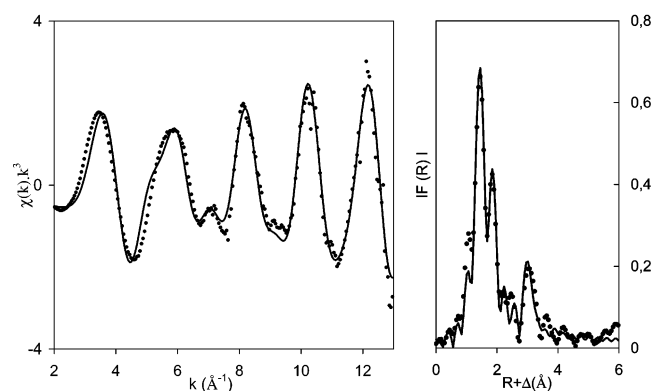
surface organometallic chemistry. The choice of tantalum for such a study has been based on its unusual reactivity toward alkanes because alkane metathesis, a reaction which transforms an alkane into its higher and lower homologues, was originally discovered with  $[(\equiv\text{SiO})_2\text{Ta}-\text{H}]$ , a  $d^2$  electron complex alkane metathesis catalyst.<sup>12</sup> We have recently disclosed that the mixture of  $[(\equiv\text{SiO})\text{Ta}(=\text{CH}t\text{Bu})(\text{CH}_2t\text{Bu})_2]$  (**1a**) and  $[(\equiv\text{SiO})_2\text{Ta}(=\text{CH}t\text{Bu})(\text{CH}_2t\text{Bu})]$  (**1b**), both  $d^0$  electron complexes, is also a catalyst precursor for this reaction.<sup>13</sup> Because this study yielded two well-defined complexes, their activity in alkane metathesis was tested to gather information on the key requirements for an alkane metathesis catalyst precursors.

## Results and Discussion

**Reactivity of  $[\text{Ta}(=\text{CH}t\text{Bu})(\text{CH}_2t\text{Bu})_3]$  with Silica Partially Dehydroxylated at 700 °C.** An exemplary case for multi-technique SOMC is given by the studies of the reactivity of  $[\text{Ta}(=\text{CH}t\text{Bu})(\text{CH}_2t\text{Bu})_3]$  with partially dehydroxylated silica.<sup>8,11,14,15</sup> In the specific case of a silica partially dehydroxylated at 700 °C, the reaction leads to a yellow solid **1**, whose structure can be formulated as the well-defined monosiloxy Ta<sup>V</sup> carbene  $[(\equiv\text{SiO})\text{Ta}(=\text{CH}t\text{Bu})(\text{CH}_2t\text{Bu})_2]$ , **1a**, as deduced by the combined use of mass balance analyses, IR, 1D and 2D HETCOR NMR spectroscopies (Table 1), and characterization through chemical reactivity studies (such as pseudo-Wittig or hydrolysis).

Furthermore, isotopic distribution studies<sup>14</sup> and 1D solid-state NMR spectroscopy on selectively  $^{13}\text{C}$ -labeled complexes<sup>8</sup> have indicated the involvement of the surface intermediate  $[(\equiv\text{SiO})\text{Ta}(\text{CH}_2t\text{Bu})_4]$ , **1c**, during the grafting reaction, and the slow transformation of **1c** into  $[(\equiv\text{SiO})\text{Ta}(=\text{CH}t\text{Bu})(\text{CH}_2t\text{Bu})_2]$  **1a** and neopentane. The identification and characterization of **1c**, and the related mechanism of the grafting reaction, was further substantiated by studies of the reaction of the organometallic precursor with a molecular model for silica's surface isolated grafting site, the polyhedral oligosilsesquioxane  $[(c\text{-C}_5\text{H}_9)_7\text{Si}_7\text{O}_{12}\text{Si}(\text{OH})]$ .<sup>8</sup> Studies based solely on  $^{13}\text{C}$  solid-state NMR data for this reaction have postulated the same intermediate species, although NMR data have not always been correctly assigned.<sup>11</sup>

Ideally, one would like to obtain crystallographic data to yield the interatomic geometric parameters of the coordination sphere of a metal center and its surroundings in the same way molecular chemists use X-ray crystallography diffraction studies on single crystals. In the case of silica, an amorphous support, extended X-ray absorption fine structure (EXAFS) analysis provides

**Figure 1.** EXAFS of solid **1**: dashed lines, experimental; solid lines, spherical wave theory.**Table 2.** EXAFS Parameters for Solid **1**<sup>a</sup>

neighboring atom	# of atoms <sup>b</sup>	distance (Å)	Debye–Waller factor (Å)
$=\text{CHCMe}_3$	1	1.898(8)	0.07(6)
$-\text{OSi}$	1	1.898	0.03(2)
$-\text{CH}_2\text{CMe}_3$	2	2.150(4)	0.07(2)
$-\text{OSi}_2$	1	2.64(1)	0.11(4)
$-\text{CH}_2\text{CMe}_3$	3	3.417(5)	0.06(2)

<sup>a</sup> Fit residue:  $\rho = 5.8\%$ . <sup>b</sup> All shells fit with an overall scale factor of 1.1.

insight into the number and distances of first and second neighbors. The EXAFS data collected on the solid **1** are consistent with the following features (Figure 1 and Table 2): (i) two neighbors (either carbon or oxygen atoms) at a short distance (1.898 Å, not resolved), (ii) two other carbon neighbors at a longer distance (2.150 Å), (iii) an extra oxygen atom at a much longer distance (2.64 Å), and (iv) three carbon atoms at 3.417 Å. The two neighbors at a short bond distance (1.898 Å) can be assigned to an alkylidene ( $=\text{CH}t\text{Bu}$ ) and a  $\sigma$ -bonded siloxy ( $\text{OSi}\equiv$ ) substituent, while those at 2.150 Å are assigned to two  $\sigma$ -bonded carbons of the neopentyl groups ( $\text{CH}_2t\text{Bu}$ ). The extra O-atom neighbor at 2.64 Å is assigned to a siloxane bridge which acts as a two-electron donor ligand to stabilize the otherwise highly electron unsaturated surface complex **1a** (formally a 10-electron complex) to yield the more stabilized 12-electron species  $[(\equiv\text{SiO})\text{Ta}(=\text{CH}t\text{Bu})(\text{CH}_2t\text{Bu})_2-(\equiv\text{SiOSi}\equiv)]$ , **1a'**.

The proposed ligand assignments for the observed bond distances are consistent with corresponding bond distances obtained by X-ray crystallography in analogous molecular complexes, such as  $d(\text{Ta}=\text{CH}t\text{Bu}) = 1.89$  Å,<sup>16,17</sup>  $d(\text{Ta}-\text{C}) = 2.19$  Å,<sup>18</sup>  $d(\text{Ta}-\text{OSi}) = 1.89$  Å,<sup>19</sup> and  $d(\text{Ta}\leftarrow\text{O}) = 2.25\text{--}2.35$  Å for a coordinated ether.<sup>20,21</sup>

Recently, *J*-resolved 2D solid-state NMR spectroscopy was introduced as a novel method to measure the M–C–H bond angle and was applied to the study of surface-bound metallo-

- (12) Vidal, V.; Theolier, A.; Thivolle-Cazat, J.; Basset, J.-M. *Science* **1997**, *276*, 99–102.
- (13) Copéret, C.; Maury, O.; Thivolle-Cazat, J.; Basset, J.-M. *Angew. Chem., Int. Ed.* **2001**, *40*, 2331–2334.
- (14) Dufaud, V.; Nicolai, G. P.; Thivolle-Cazat, J.; Basset, J.-M. *J. Am. Chem. Soc.* **1995**, *117*, 4288–4294.
- (15) Lefort, L.; Chabanais, M.; Maury, O.; Meunier, D.; Copéret, C.; Thivolle-Cazat, J.; Basset, J.-M. *J. Organomet. Chem.* **2000**, *593*–594, 96–100.

- (16) Schrock, R. R. *Acc. Chem. Res.* **1979**, *12*, 98–104.
- (17) Schultz, A. J.; Brown, R. K.; Williams, J. M.; Schrock, R. R. *J. Am. Chem. Soc.* **1981**, *103*, 169–176.
- (18) LaPointe, R. E.; Wolczanski, P. T.; Van Duyne, G. D. *Organometallics* **1985**, *4*, 1810–1818.
- (19) Miller, R. L.; Toreki, R.; LaPointe, R. E.; Wolczanski, P. T.; Van Duyne, G. D.; Roe, D. C. *J. Am. Chem. Soc.* **1993**, *115*, 5570–5588.
- (20) Allen, K. D.; Bruck, M. A.; Gray, S. D.; Kingsborough, R. P.; Smith, D. P.; Weller, K. J.; Wigley, D. E. *Polyhedron* **1995**, *14*, 3315–3333.
- (21) Bott, S. G.; Sullivan, A. C. *J. Chem. Soc., Chem. Commun.* **1988**, 1577–1578.

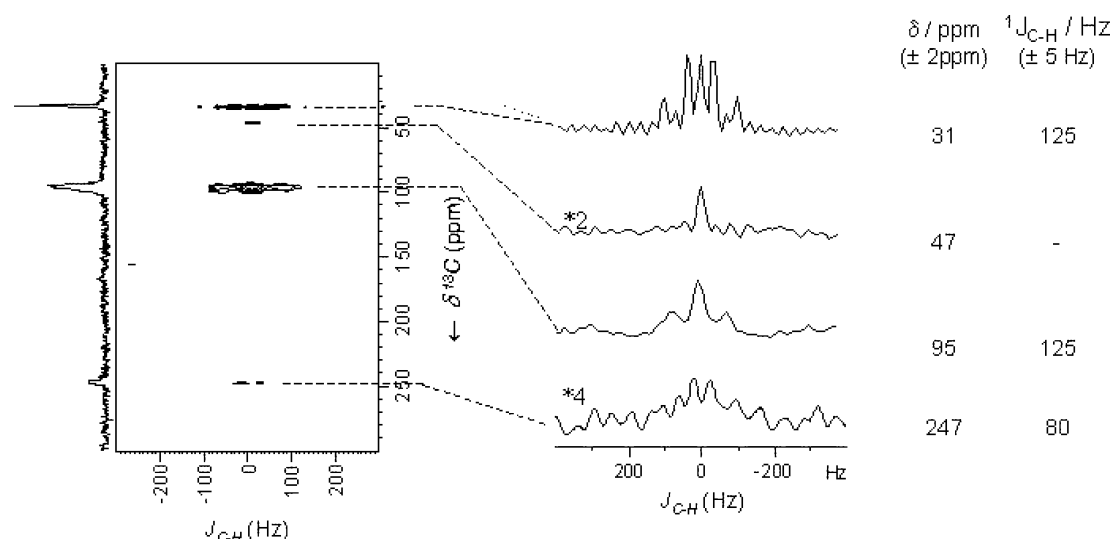
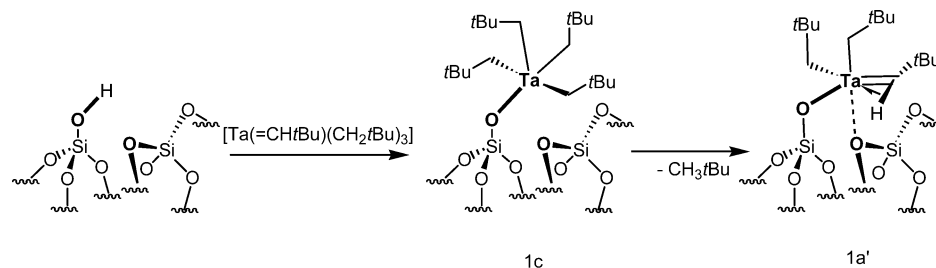


**Figure 2.** 2D  $J$ -resolved solid-state NMR spectrum of solid **1**, 10%  $^{13}\text{C}$  enriched at the  $\alpha$  positions (\*). Traces extracted along the  $\omega_1$  dimension of the 2D  $J$ -resolved spectrum at different carbon chemical shift frequencies: 31, 47, 95, and 247 ppm.

**Scheme 1.** Reactivity of  $[\text{Ta}(\text{=CHtBu})(\text{CH}_2\text{tBu})_3]$  with  $\text{SiO}_2\text{--}(700)$ : Formation of  $[\text{=SiO--Ta}(\text{=CHtBu})(\text{CH}_2\text{tBu})_2(\text{=SiOSi=})]$  (**1a'**)



carbenes<sup>9</sup> because their  $J(\text{C--H})$  coupling constant is strongly correlated with this angle.<sup>16,22,23</sup>

The results of the  $J$ -resolved 2D solid-state NMR study of **1a'** are reported in Table 2 and Figure 2.

The carbenic signal at 247 ppm appears as a doublet with a very small coupling constant of  $^1J_{\text{C--H}} = 80$  Hz, strongly indicating that the C--H bond is stretched and that the Ta--C--H bond angle is very acute (probably lower than  $90^\circ$ ). Similarly, the molecular silsesquioxane analogue,  $[(\text{c-C}_5\text{H}_9)_7\text{Si}_7\text{O}_{12}\text{SiO}]\text{Ta}(\text{=CHtBu})(\text{CH}_2\text{tBu})_2$  (**1m**), also displays a doublet ( $J_{\text{C--H}} = 86$  Hz) at 245 ppm assigned to its carbenic carbons. Because similar spectroscopic features have been observed for the starting molecular complex, and explained in terms of an agostic interaction between the metallic center and the carbenic proton,<sup>16,24--26</sup> we propose that the same type of agostic interaction is also present for the surface-bound Ta center and its  $\alpha$ -carbenic proton of **1a'**.

The signal at 95 ppm, assigned to methylene ( $\text{CH}_2\text{tBu}$ ), is a triplet, with C--H coupling constant  $^1J_{\text{C--H}} = 125$  Hz, as expected for an  $\text{sp}^3$  carbon. The molecular complex **1m** exhibits the analogous signal at 98.7 ppm (triplet,  $^1J_{\text{C--H}} = 109$  Hz). In addition, there is a sharp singlet at 40 ppm, which can be

assigned to the quaternary carbon of the tertbutyl group attached to the carbene ligand; one other multiplet can be observed at 30 ppm, this resonance corresponding probably to the superimposition of a quadruplet ( $^1J_{\text{C--H}} = 125$  Hz) due to the methyl signals and a singlet due to the quaternary carbon of the neopentyl ligands.

The combined use of EXAFS, IR, mass balance analyses, NMR studies (including  $^1J_{\text{C--H}}$ -resolved data), and studies with molecular analogues yields a sharp description of the grafting reaction of organometallic precursor  $[\text{Ta}(\text{=CHtBu})(\text{CH}_2\text{tBu})_3]$  on a silica surface (see Scheme 1).

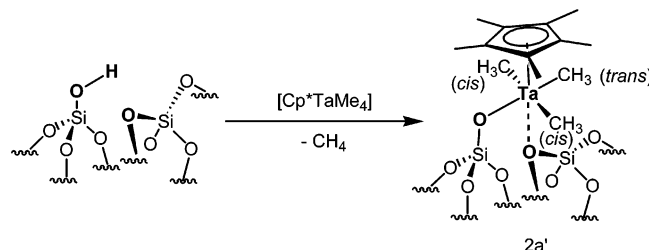
Particularly noteworthy, the EXAFS and  $J$ -resolved studies have highlighted the presence of stabilizing interactions at the Ta-center, beside the  $\sigma$ -bonded alkyl and alkylidene ligands, with which the tantalum center (formally a tetracoordinated 10-electron species, **1a**) achieves a pseudo-octahedral geometry through (i) a 2-electron donor interaction with an adjacent ( $\text{=SiOSi=}$ ) surface bridge, and (ii) an agostic interaction with the carbenic C--H bond, to yield the stabilized formally 14-electron species,  $[(\text{=SiO})\text{Ta}(\text{=CHtBu})(\text{CH}_2\text{tBu})_2(\text{=SiOSi=})]$ , **1a'**.

**Reactivity of  $[\text{Cp}^*\text{TaMe}_4]$  with Silica Partially Dehydroxylated at 700 °C.** The reports available on the reactivity of  $\text{Cp}^*\text{TaMe}_4$  (Scheme 2) with partially dehydroxylated silica are comprised of spectroscopic  $^1\text{H}$ - and  $^{13}\text{C}$ -CP NMR studies.<sup>11</sup> The data suggest that the organometallic surface species  $[(\text{=SiO})\text{TaCp}^*\text{Me}_3]$ , **2a**, is obtained, either by reaction with surface silanol [ $\text{=SiOH}$ ] and elimination of methane, or by cleavage of a surface siloxy bridge [ $\text{=SiOSi=}$ ] and formation

- (22) Brookhart, M.; Green, M. L. H. *J. Organomet. Chem.* **1983**, 250, 395–408.
- (23) Nugent, W. A.; Mayer, J. M. *Metal–Ligand Multiple Bond*; Wiley: New York, 1988.
- (24) Schultz, A. J.; Williams, J. M.; Schrock, R. R.; Rupprecht, G. A.; Fellmann, J. D. *J. Am. Chem. Soc.* **1979**, 101, 1593–1595.
- (25) Goddard, R. J.; Hoffmann, R.; Jemmis, E. D. *J. Am. Chem. Soc.* **1980**, 102, 7667–7676.
- (26) Fellmann, J. D.; Schrock, R. R.; Traficante, D. D. *Organometallics* **1982**, 1, 481–484.



**Scheme 2.** Reactivity of  $[\text{Cp}^*\text{Ta}(\text{CH}_3)_4]$  with  $\text{SiO}_2-(700)$ : Formation of  $[\text{SiO}-\text{Ta}(\text{CH}_3)_3\text{Cp}^*(\text{SiOSi})]$  (**2a'**)



of silicon bound methyl moiety,  $[\text{Si}-\text{Me}]$ . The presence of this latter species is inferred by one signal at  $-6$  ppm in the  $^{13}\text{C}$  NMR spectrum.<sup>11</sup>

Herein is discussed in detail the reaction of  $[\text{Cp}^*\text{TaMe}_4]$  with a silica partially dehydroxylated at  $700^\circ\text{C}$ . First, a silica disk partially dehydroxylated at  $700^\circ\text{C}$  ( $\text{SiO}_2-(700)$ ) was immersed at room temperature in a yellow pentane solution of  $[\text{Cp}^*\text{TaMe}_4]$  (1.2 equiv/surface silanols;  $0.26 \pm 0.03$  mmol accessible OH/g). After the excess molecular complex was washed and the resulting solid was dried under dynamic vacuum ( $10^{-5}$  Torr, 2 h), an IR spectrum was recorded (Figure 3).

The narrow band assigned to isolated silanols at  $3747\text{ cm}^{-1}$  totally disappeared, leaving a broad band in the  $3740\text{--}3550\text{ cm}^{-1}$  region as well as two sets of bands in the  $3000\text{--}2700$  and  $1500\text{--}1300\text{ cm}^{-1}$  regions. The broad band corresponds to  $\nu_{(\text{O}-\text{H})}$  of residual silanols in interaction with the perhydrocarbyl ligands present at the surface of silica (vide infra for further comments), the two latter sets of IR bands being assigned to  $\nu_{(\text{CH})}$  and  $\nu_{(\text{C}=\text{C})}/\delta_{(\text{CH})}$  vibrations.

Second, using larger quantities of silica (0.20–1.0 g) allowed the methane released to be quantified: 1.1–1.2 equiv of methane was evolved per grafted Ta, consistent with a chemical grafting of the molecular complex. This reaction occurs via cleavage of one  $(\text{Ta}-\text{CH}_3)$  bond by a surface silanol forming a covalent  $(\text{Ta}-\text{Osi})$  bond and methane to yield a yellow solid **2**. The formation of  $[(\text{SiO})\text{TaCp}^*\text{Me}_3]$ , **2a**, leads to 1 mol of MeH/mol of grafted Ta as expected, and therefore small quantities of the bisiloxy species  $[(\text{SiO})_2\text{TaCp}^*\text{Me}_2]$ , **2b**, for which 2 mol of MeH/mol of grafted Ta are expected, could also be possibly formed. Elemental analysis of the yellow solid shows the presence of  $12 \pm 2$  carbons/Ta, which is consistent with the proposed structure (13 C/Ta and 12 C/Ta for **2a** and **2b**, respectively). The tantalum loading typically varies between 2.6 and 3.7 Ta % wt, depending on the batch of  $\text{SiO}_2-(700)$  used (depending on how much silica was compacted). Such tantalum loadings correspond to 0.14–0.21 mmol of Ta/g of solid, while  $\text{SiO}_2-(700)$  typically contains  $0.26 \pm 0.03$  mmol of OH/g on silica. Therefore, such low loading indicates a partial consumption of the surface silanols as already evidenced by in situ IR experiments (vide supra) where a broad band assigned to residual silanols was detected. This is in contrast to what has been observed in the reaction of  $[\text{Ta}(\text{CH}_2\text{tBu})(\text{CH}_2\text{tBu})_3]$  with  $\text{SiO}_2-(700)$ ,<sup>15</sup> for which all surface silanols are consumed, but it is consistent with the larger size of the  $[\text{TaCp}^*\text{Me}_3]$  fragment as compared to that of  $[\text{Ta}(\text{CH}_2\text{tBu})(\text{CH}_2\text{tBu})_2]$ , which, in turn, would prevent the access of the molecular complex,  $[\text{Cp}^*\text{TaMe}_4]$ , to the remaining surface silanols.

Third, the solid-state  $^1\text{H}$  MAS NMR spectrum of the yellow solid **2** shows an intense peak at 1.61 ppm along with broad signals between  $-0.3$  and  $0.7$  ppm, as does the  $^1\text{H}$  spectrum of

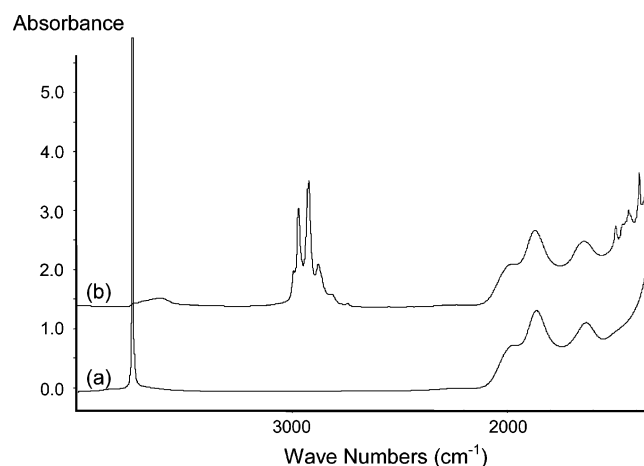


**Figure 3.** IR spectra of the reaction of  $[\text{Cp}^*\text{Ta}(\text{CH}_3)_4]$  with  $\text{SiO}_2-(700)$  by IR spectroscopy: (a)  $(\text{SiO}_2-(700))$  and (b)  $[\text{SiO}-\text{Ta}(\text{CH}_3)_3\text{Cp}^*(\text{SiOSi})]$ .

its  $^{13}\text{C}$ -labeled (20% on the Me substituents attached to Ta) analogue, **2\*** (Figure 4a). The  $^{13}\text{C}$  CP/MAS NMR spectrum of **2** displays three signals at 117, 58, and 9 ppm, as does the spectrum of **2\*** (albeit with different relative ratios, Figure 4b). In accord with the literature data,<sup>11</sup> the signals at 117 and 9 ppm can be tentatively assigned to the carbons of the cyclopentadienyl ring and the methyl groups of the  $\text{Cp}^*$  ligand, respectively, and the signal at 58 ppm can be assigned to that of the  $(\text{Ta}-\text{Me}_3)$  groups, which is shifted upfield as compared to that of the starting molecular complex  $[\text{Cp}^*\text{TaMe}_4]$  ( $\text{Ta}-\text{Me}_4$ , 74 ppm). The large upfield shift in going from a molecular to a supported complex is consistent with the replacement of one methyl group by an electronegative siloxy group.<sup>27,28</sup> No resonance of any significance could be detected at  $-6$  ppm, which is the signature peak of  $[\text{Si}-\text{Me}]$  as previously reported,<sup>11</sup> and no further evidence for a bisiloxy species could be obtained through these NMR studies.

Fourth, the 2D  $^1\text{H}-^{13}\text{C}$  HECTOR NMR spectrum of **2\***, recorded with a contact time of 1 ms (Figure 4c), shows a correlation between the signal at 1.6 ppm in the  $F_1$  dimension ( $^1\text{H}$ ) and the signal at 9 ppm in the  $F_2$  dimension ( $^{13}\text{C}$ ), which are assigned to the methyl groups of the pentamethylcyclopentadienyl ring. The  $^{13}\text{C}$  resonance of the methyl groups directly bonded to the tantalum gives two pairs of correlations:  $-0.05$  ppm/58.0 ppm and  $-0.28$  ppm/57.5 ppm in the  $F_1/F_2$  dimensions. These two types of proton–carbon resonances probably correspond to the methyl group trans to oxygen (58.0 and  $-0.05$  ppm), and the other correlation (57.5 and  $-0.28$  ppm) corresponds to the cis methyl groups as observed for similar molecular complexes,  $\text{Cp}^*\text{TaXMe}_3$  ( $\text{X} = \text{Cl}, \text{OMe}, \text{OiPr}, \text{OtBu}, \text{NMe}_2$ ), which adopt a “four-legged piano stool” geometry and in which the two types of methyl groups are not equivalent.<sup>27</sup> The signal at 0.6 ppm in the  $F_1$  dimension ( $^1\text{H}$ ) does not correlate with any carbon (in the  $F_2$  dimension), and this signal disappears when using deuterated silica (see Supporting Information). Therefore, the resonance at 0.6 ppm is most likely due to a surface silanol  $[\text{SiO}-\text{H}]$  resonance, which is shifted upfield

(27) Mayer, J. M.; Curtis, C. J.; Bercaw, J. E. *J. Am. Chem. Soc.* **1983**, *105*, 2651–2660.

(28) Gomez, M.; Jimenez, G.; Royo, P.; Selas, J. M.; Raithby, P. R. *J. Organomet. Chem.* **1992**, *439*, 147–154.

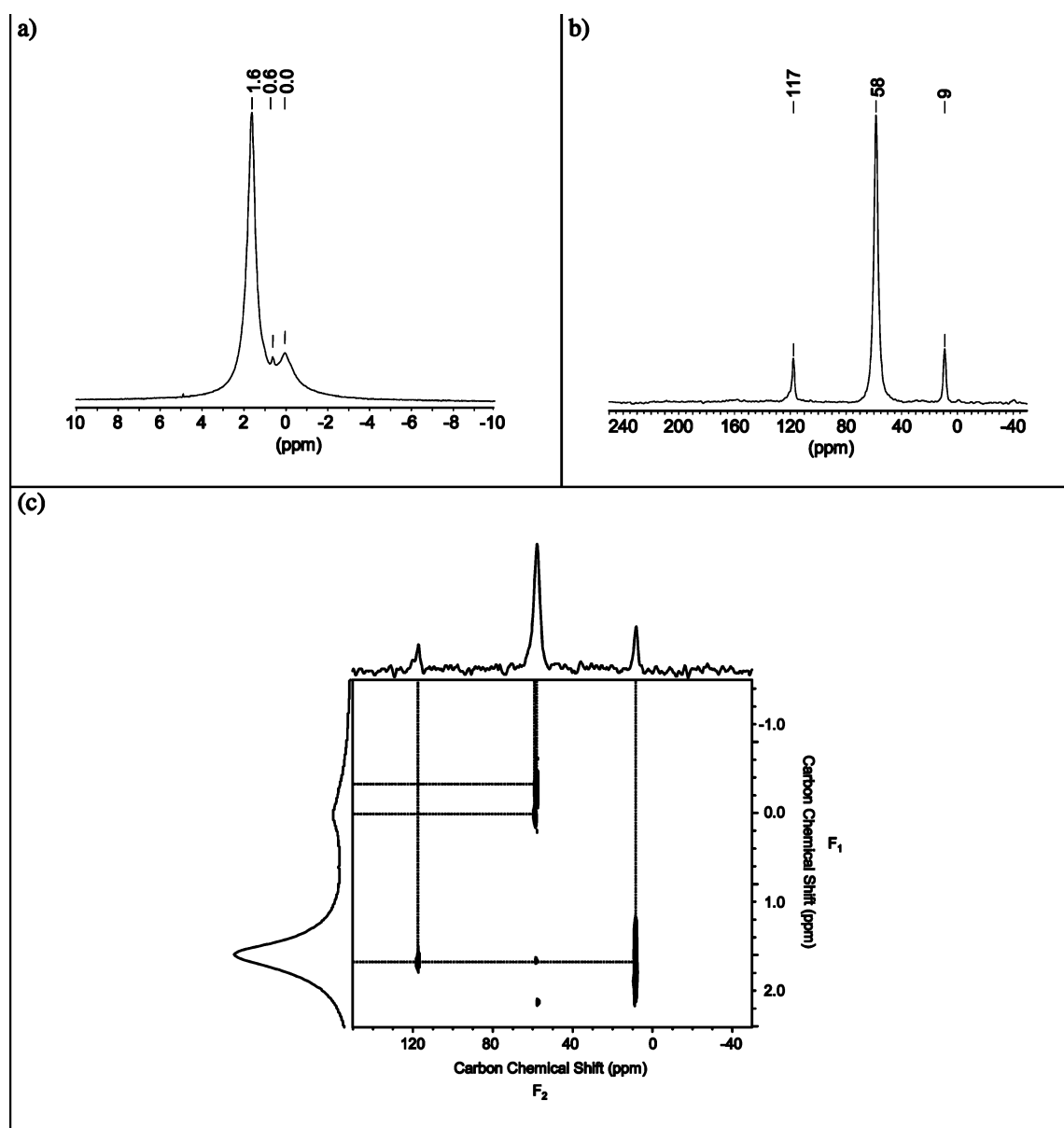


**Figure 4.** (a)  $^1\text{H}$  MAS NMR spectrum of **2\*** (number of scans = 8, repetition delay = 8 s,  $90^\circ$  H pulse =  $3\ \mu\text{s}$ , no apodization). (b)  $^{13}\text{C}$  CP/MAS spectrum of **2\*** (number of scans = 78 339, repetition delay = 2 s,  $\text{P15} = 5\ \text{ms}$ , line broadening = 100 Hz). (c) 2D HETCOR solid-state NMR spectroscopy on **2\***. The displayed spectra correspond to a  $^1\text{H}$  MAS NMR spectrum (number of scans = 16, repetition delay = 8 s, line broadening = 5 Hz) for  $F_1$  and  $^{13}\text{C}$  CP/MAS spectrum (number of scans = 1024, repetition delay = 2 s,  $\text{P15} = 1\ \text{ms}$ , line broadening = 80 Hz) for  $F_2$ .

with respect to the silanols of silica (typically observed at 1.8 ppm), most likely because of a ring-current effect of the adjacent  $\text{Cp}^*$  ring.

Finally, Tantalum  $L_{\text{III}}$ -edge EXAFS measurements on **2** provided further insight into the structure of this silica-supported Ta species (Figure 5).

The data are consistent with an average of 1.3 oxygen atoms at 1.931 Å, 2.7 carbon atoms at 2.142 Å, and 5.0 carbon atoms at 2.456 Å in the coordination sphere of Ta, which is in turn consistent with **2a** being the major species present in the solid, and **2b** (if any) as a minor product (Table 3).

The proposed assignment for measured Ta–C bond distances is in good agreement with values obtained from crystallographic data for Ta–C(Me) (2.074–2.150 Å in  $[\text{TaMe}_5]$ ;<sup>29</sup> 2.115 Å in

$[\text{TaMe}_3(\text{OAr})_2]$ ;<sup>30</sup> 2.181 Å in  $[\text{Cp}^*\text{TaMe}_2(\text{C}_6\text{H}_4)]$ ;<sup>31</sup> and 2.22–2.26 Å in  $[(\text{TaMe}_3\text{Cp}^*)_2(\mu\text{-O})]$ <sup>32</sup>) and Ta–C(pentamethylcyclopentadienyl) distances (2.345–2.406 Å in  $[\text{Cp}^*\text{TaCl}_2\text{Me}_2]$ ;<sup>28</sup> 2.424–2.480 Å in  $[\text{Cp}^*\text{Ta}(p\text{-tert-butylcalix[4]arene})]$ ;<sup>33</sup> 2.366–2.518 Å in  $[\text{Cp}^*\text{Ta}(=\text{NAr})\text{Cl}_2]$ <sup>34</sup>). Moreover, the agreement with the EXAFS data was improved when the model included five carbons at 3.44 Å, corresponding to the five methyl groups of the  $\text{Cp}^*$  ligand (3.42–3.61 Å in  $[\text{Cp}^*\text{Ta}(=\text{NAr})\text{Cl}_2]$ <sup>34</sup>), and an extra 1.3 oxygen atoms at 3.04 Å, which can be assigned to that of siloxane bridges close to a tantalum species, to yield

(30) Chamberlain, L. R.; Rothwell, I. P.; Huffman, J. C. *J. Am. Chem. Soc.* **1986**, *108*, 1502–1509.

(31) Churchill, M. R.; Youngs, W. J. *Inorg. Chem.* **1979**, *18*, 1697–1702.

(32) Jernakoff, P.; De Meric de Bellefon, C.; Geoffroy, G. L.; Rheingold, A. L.; Geib, S. J. *Organometallics* **1987**, *6*, 1362–1364.

(33) Acho, J. A.; Doerrer, L. H.; Lippard, S. J. *Inorg. Chem.* **1995**, *34*, 2542–2556.

(34) Gavenonis, J.; Tilley, T. D. *Organometallics* **2004**, *23*, 31–43.

(29) Roessler, B.; Kleinhenz, S.; Seppelt, K. *Chem. Commun.* **2000**, 1039–1040.

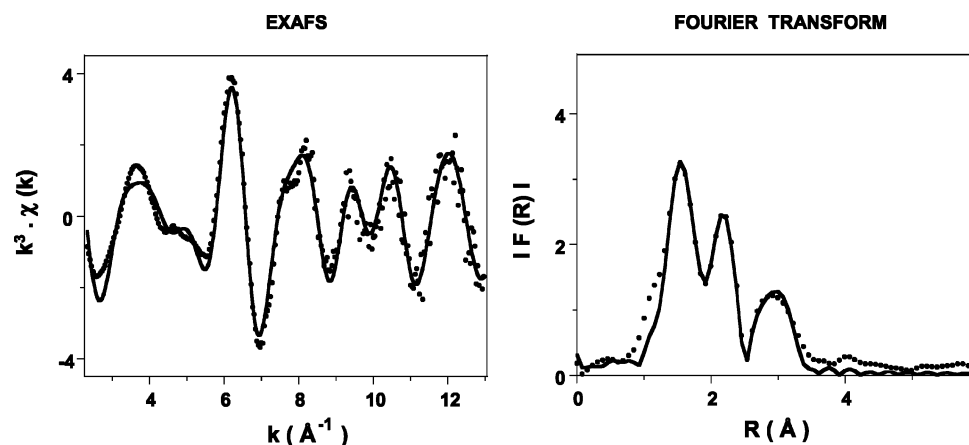


**Figure 5.** Ta L<sub>III</sub>-edge  $k^3$ -weighted EXAFS (left) and Fourier transform (right) of **2**. Dashed lines, experimental; solid lines, spherical wave theory.

**Table 3.** EXAFS Parameters for Solid **2**<sup>a</sup>

neighboring atom	# of atoms	distance from Ta (Å)	Debye–Waller factor (Å)
OSi	1.3	1.931	0.042
CH <sub>3</sub>	2.7	2.142	0.097
C' (Cp* ring)	5.0	2.456	0.086
OSi <sub>2</sub>	1.3	3.040	0.063
C'' (Me of Cp*)	4.8	3.445	0.082

<sup>a</sup> Fit residue:  $\rho = 7.8\%$ .

[( $\equiv$ SiO)TaCp\*Me<sub>3</sub>( $\equiv$ SiOSi $\equiv$ )], **2a'**, analogous to the observations for the carbenic derivative discussed above [( $\equiv$ SiO)Ta( $\equiv$ CH*t*Bu)(CH<sub>2</sub>*t*Bu)<sub>2</sub>( $\equiv$ SiOSi $\equiv$ )], **1a'**.

In summary, the combined analysis of the experimental data collected on the reaction of Cp\*TaMe<sub>4</sub> with SiO<sub>2</sub>-(700) indicates the presence of [( $\equiv$ SiO)TaMe<sub>3</sub>Cp\*( $\equiv$ SiOSi $\equiv$ )] (**2a'**) as a major species, in which a siloxane bridge acts as an extra donor ligand to the Ta center. In contrast to most organometallic complexes studied so far, only part of the surface silanols reacted with [Cp\*TaMe<sub>4</sub>], as demonstrated by elemental analysis, IR, and NMR spectroscopies. The remaining silanols interact with a nearby Cp\* as observed through the upfield shift of  $\delta$ ( $\equiv$ SiOH) in the <sup>1</sup>H NMR spectrum. The grafting mechanism corresponds to the silanolysis of a Ta–Me bond by a surface [ $\equiv$ SiOH], with elimination of 1 mole of methane, while no evidence was obtained supporting the previously proposed addition of a Ta–C across a Si–O bond of a surface siloxy bridge [ $\equiv$ SiOSi $\equiv$ ].<sup>11</sup>

**Comparison of the Reactivity of [Cp\*TaMe<sub>4</sub>] and [Ta( $\equiv$ CH*t*Bu)(CH<sub>2</sub>*t*Bu)<sub>3</sub>] Supported on Silica Partially Dehydroxylated at 700 °C toward Propane.** In the case of [( $\equiv$ SiO)Ta(CH<sub>3</sub>)<sub>3</sub>Cp\*( $\equiv$ SiOSi $\equiv$ )] (**2a'**), a sterically crowded electron-rich Ta<sup>V</sup> surface complex, its reaction with propane yields methane as the sole gaseous product, which probably formed via the decomposition of **2a'** (Table 4). On the other hand, [( $\equiv$ SiO)Ta( $\equiv$ CH*t*Bu)(CH<sub>2</sub>*t*Bu)<sub>2</sub>( $\equiv$ SiOSi $\equiv$ )] (**1a'**), an electron-deficient Ta<sup>V</sup> surface complex as evidenced by the C–H agostic interaction, catalytically transforms propane into its higher and lower homologues (Table 4). Moreover, initiation products, which result from the reaction of the neopentyl/neopentylidene fragments in **1a'** and propane, are also formed: 2,2-dimethylpropane (*t*BuCH<sub>2</sub>-H, 1.05 equiv/Ta), 2,2-dimethylbutane (*t*BuCH<sub>2</sub>-CH<sub>3</sub>, 0.30 equiv/Ta), and 2,2-dimethylpentane (*t*BuCH<sub>2</sub>-CH<sub>2</sub>CH<sub>3</sub>, 0.11 equiv/Ta). Note that no *t*BuCH<sub>2</sub>-CH<sub>2</sub>CH<sub>2</sub>CH<sub>3</sub> (<0.1%, not detected) is formed. The ratio of initiation products *t*BuCH<sub>2</sub>-CH<sub>3</sub>/*t*BuCH<sub>2</sub>-CH<sub>2</sub>CH<sub>3</sub> is 2.5. Simi-

**Table 4.** Reactivity of Tantalum Species Supported on Silica toward Propane

catalysts	% wt Ta	P (Torr)	ratio (nC <sub>3</sub> H <sub>8</sub> /nTa)	conv. <sup>a</sup> (%)	TON <sup>a</sup> (mol P/mol Ta)
solid <b>2</b>	3.5	495	805	0	0
solid <b>1</b>	3.9	600	580	5.8	33–34 <sup>b</sup>
[( $\equiv$ SiO) <sub>2</sub> Ta–H]	5.0	550	1065	6.1	65 <sup>c</sup>

<sup>a</sup> As measured after 120 h. <sup>b</sup> The selectivities in methane, ethane, isobutane, butane, isopentane, pentane, and hexanes are 12.8%, 47.7%, 10.2%, 22.2%, 2.5%, 3.6%, and 0.9%, respectively. <sup>c</sup> The selectivities in methane, ethane, isobutane, butane, isopentane, pentane, and hexanes are 18.0%, 40.0%, 8.6%, 24.4%, 2.9%, 5.1%, and 1%, respectively.

larly in olefin metathesis (Scheme 3), we have observed the initiation products of the reaction of propene and [( $\equiv$ SiO)Re( $\equiv$ CH*t*Bu)( $\equiv$ CH*t*Bu)(CH<sub>2</sub>*t*Bu)( $\equiv$ SiOSi $\equiv$ )]: *t*BuCH=CH<sub>2</sub> and *trans-t*BuCH=CHCH<sub>3</sub> (no *cis-t*BuCH=CHCH<sub>3</sub> is detected).<sup>35,36</sup> Their ratio (*t*BuCH=CH<sub>2</sub>/*trans-t*BuCH=CHCH<sub>3</sub>) is 3.0, which is closely related to that observed for the initiation products in the metathesis of propane on [( $\equiv$ SiO)Ta( $\equiv$ CH*t*Bu)(CH<sub>2</sub>*t*Bu)<sub>2</sub>( $\equiv$ SiOSi $\equiv$ )] (**1a'**). In this latter case, the selectivity in initiation products can be understood in terms of minimization of the steric interactions in the metallacyclobutane intermediates (or in their formation),<sup>37</sup> which is governed by the relative position of the substituents: typically substituents in the [1,3]-positions (usually both in equatorial positions) of the metallacyclobutane intermediate generate less steric hindrance than those in the [1,2]-positions (usually both in equatorial positions, Scheme 3).<sup>38</sup>

The selectivity in propane metathesis can also be explained by using the same model in which [1,3]- and [1,2]-interactions determine the ratio of products. For instance, the butane/pentane ratios are 6.2 and 4.8 for **1a'** and [( $\equiv$ SiO)<sub>2</sub>Ta–H], respectively (Table 4).<sup>39</sup> A similar trend is observed for the isobutane/isopentane ratios, which are 4.1 and 3.0, respectively. The higher selectivity in butanes (the transfer of one carbon via metallacyclobutanes involving [1,3]-interactions) than that of pentanes

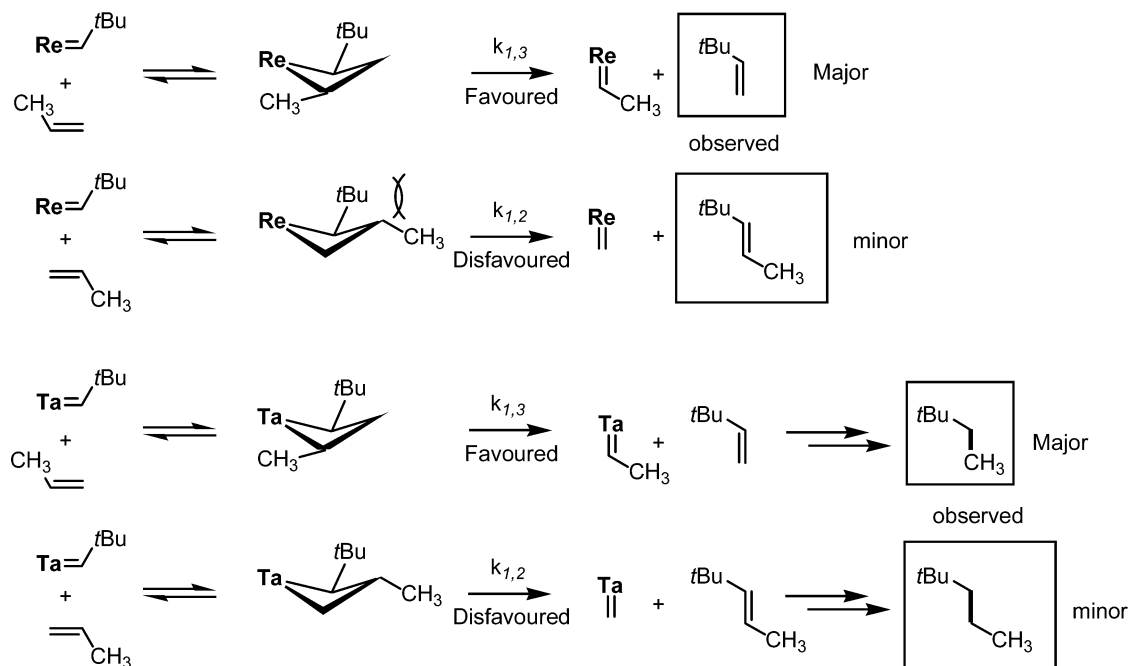
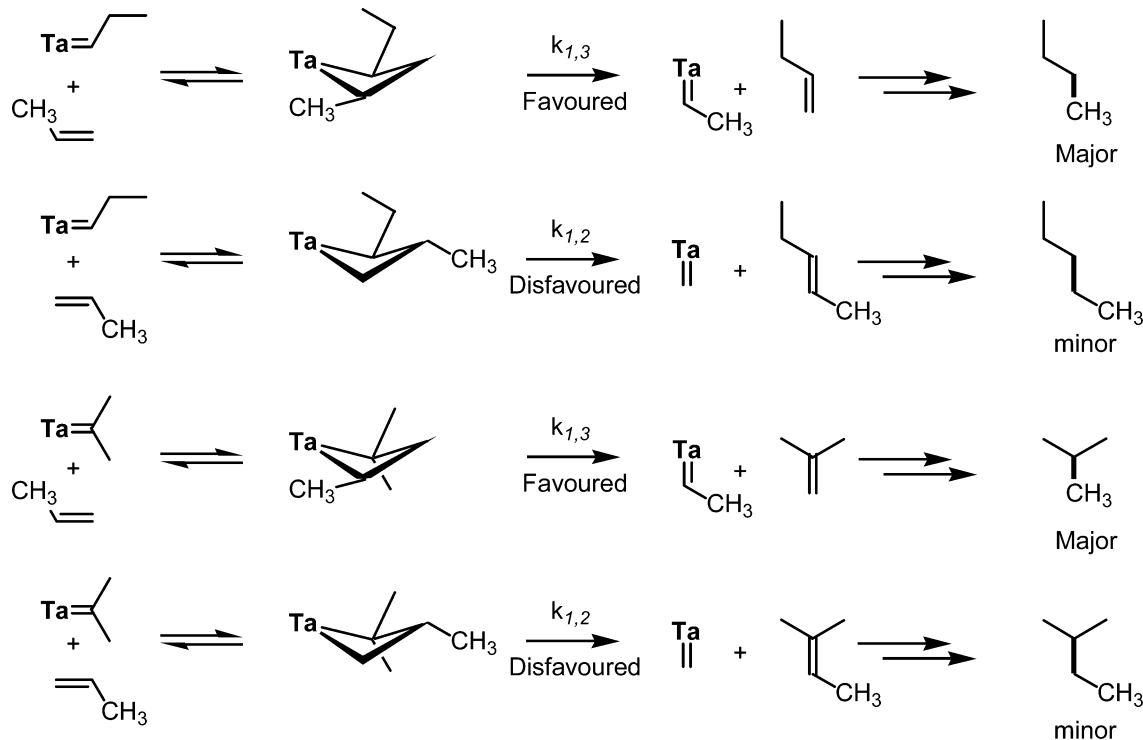
(35) Chabanas, M.; Baudouin, A.; Copéret, C.; Basset, J.-M. *J. Am. Chem. Soc.* **2001**, *123*, 2062–2063.

(36) Chabanas, M.; Copéret, C.; Basset, J.-M. *Eur. J. Chem.* **2003**, *9*, 971–975.

(37) Wallace, K. C.; Dewan, J. C.; Schrock, R. R. *Organometallics* **1986**, *5*, 2162–2164.

(38) Bilhou, J. L.; Basset, J. M.; Mutin, R.; Graydon, W. F. *J. Am. Chem. Soc.* **1977**, *99*, 4083–4090.

(39) In the case of Ta–H, this ratio does not change with time, while the isobutane/butane ratio decreases in the case of [( $\equiv$ SiO)Ta( $\equiv$ CH*t*Bu)(CH<sub>2</sub>*t*Bu)<sub>2</sub>] because isobutane is also formed through the decomposition of this complex at 150 °C.

**Scheme 3.** Possible Relation between the Mechanisms of Olefin and Alkane Metatheses: The Initiation Step

**Scheme 4.** Model for Product Selectivities in Alkane Metathesis


(the transfer of two carbons via metallacyclobutanes involving [1,2]-interactions) is consistent with this model (Schemes 3 and 4).

Because alkane metathesis catalysts need to be highly electrophilic and coordinatively unsaturated ( $\text{Cp}^*$  is detrimental to catalysis), because the selectivities of initiation products and alkane metathesis products are similar to that observed for olefin metathesis, and because **1a'**, a metalcarbene, is a catalyst precursor for alkane metathesis, we therefore propose that one of the key steps in alkane metathesis would be the formation of a metallacyclobutane intermediate and probably involves

metallocarbenes rather than direct C–C  $\sigma$ -bond metathesis or oxidative addition pathways as was suggested earlier as a possible working hypothesis.

## Experimental Details

**General Procedure.** All experiments were carried out under a controlled atmosphere, using Schlenk and glovebox techniques for the organometallic synthesis. For the synthesis and treatments of the surface species, reactions were carried out using high-vacuum lines (1.34 Pa) and glovebox techniques.  $\text{SiO}_2$  (Aerosil Degussa,  $200 \text{ m}^2 \text{ g}^{-1}$ ) was compacted with distilled water, calcined ( $500^\circ\text{C}$  under air for 4 h),



and partially dehydroxylated under vacuum (1.34 Pa) at 500 °C for 12 h and then at 700 °C for 4 h (support referred to as SiO<sub>2</sub>-(700)). [Ta(=CHtBu)(CH<sub>2</sub>tBu)<sub>3</sub>] and [Cp\*Ta(CH<sub>3</sub>)<sub>3</sub>] were prepared according to the literature procedure.<sup>40</sup> The 10% <sup>13</sup>C-labeled [Ta(=CHtBu)(CH<sub>2</sub>tBu)<sub>3</sub>] was prepared as reported previously.<sup>8,10</sup> <sup>13</sup>C-labeled Cp\*Ta(CH<sub>3</sub>)<sub>3</sub> was prepared following the literature procedure for the unlabeled complex, using <sup>13</sup>CH<sub>3</sub>Li prepared from Li wire and CH<sub>3</sub>I.<sup>41</sup> Pentane and diethyl ether were distilled on NaK alloy and Na/benzophenone, respectively followed by degassing through freeze–pump–thaw cycles. Infrared spectra were recorded on a Nicolet Magna 550 FT spectrometer equipped with a cell designed for in situ reactions under controlled atmosphere. Elemental analyses were performed at the Service Central d'Analyses of CNRS in Solaize.

<sup>1</sup>H MAS and <sup>13</sup>C CP-MAS solid-state NMR spectra were recorded on a Bruker DSX-300 spectrometer. For specific studies (see below), <sup>1</sup>H MAS and <sup>13</sup>C CP-MAS solid-state NMR spectra were recorded on Bruker Avance-500 spectrometers with a conventional double resonance 4 mm CP-MAS probe at the Laboratoire de Chimie in Ecole Normale Supérieure de Lyon or at the Laboratoire de Chimie Organometallique de Surface in Ecole Supérieure de Chimie Physique Electronique de Lyon. The samples were introduced under Ar in a zirconia rotor, which was then tightly closed. In all experiments, the rotation frequency was set to 10 kHz unless otherwise specified. Chemical shifts were given with respect to TMS as external references for <sup>1</sup>H and <sup>13</sup>C NMR.

**Heteronuclear Correlation Spectroscopy.** The two-dimensional heteronuclear correlation experiment was performed according to the following scheme: 90° proton pulse, *t*<sub>1</sub> evolution period, cross-polarization (CP) to carbon spins, detection of carbon magnetization. For the CP step, a ramp radio frequency (RF) field<sup>42,43</sup> centered at 60 kHz was applied on protons, while the carbon RF field was matched to obtain optimal signal. The contact time for CP was set to 1 ms. During acquisition, the proton decoupling field strength was set to 83 kHz (TPPM decoupling<sup>44</sup>). A total of 32 *t*<sub>1</sub> increments with 1024 scans each were collected. The spinning frequency was 10 kHz, and the recycle delay was 1 s (total acquisition time of 9 h). Quadrature detection in *ω*<sub>1</sub> was achieved using the TPPI method.<sup>45</sup>

**J-Resolved Spectroscopy.** The two-dimensional *J*-resolved experiment was performed as previously described:<sup>9</sup> after cross-polarization from protons, carbon magnetization evolves during *t*<sub>1</sub> under proton homonuclear decoupling. Simultaneous 180° carbon and proton pulses are applied in the middle of *t*<sub>1</sub> to refocus the carbon chemical shift evolution while retaining the modulation by the heteronuclear *J*<sub>CH</sub> scalar couplings. A Z-filter is finally applied to allow phase-sensitive detection in *ω*<sub>1</sub>. Proton homonuclear decoupling was performed by using the frequency-switched Lee–Goldburg (FSLG) decoupling sequence.<sup>46,47</sup> Quadrature detection in *ω*<sub>1</sub> was achieved using the TPPI method.<sup>45</sup> The rotor spinning frequency was 10.2 kHz to synchronize the *t*<sub>1</sub> increment with the rotor period. The proton RF field strength was set to 83 kHz during *t*<sub>1</sub> (FSLG decoupling) and acquisition (TPPM decoupling).<sup>44</sup> The lengths of carbon and proton 180° pulses were 7 and 6 μs, respectively. An experimental scaling factor, measured as already described,<sup>48</sup> of 0.52 was found, which gave a corrected spectral width of 2452 Hz in

the *ω*<sub>1</sub> dimension. The recycle delay was 1.3 s, and a total of 80 *t*<sub>1</sub> increments with 1024 scans each were collected (total acquisition time = 30 h).

**Extended X-ray Absorption Fine Structure Spectroscopy (EXAFS).** EXAFS on **1a** was carried out at the Stanford Synchrotron Radiation Laboratory (SSRL) at beamline 4-1 as previously reported.<sup>10</sup> Samples **2** was packaged within an argon-filled drybox in double airtight sample holders equipped with Kapton windows. X-ray absorption spectra were acquired at the Laboratoire pour l'Utilisation du Rayonnement Electromagnétique (LURE in Orsay, France), on the DCI ring at beam line D44. They were recorded at room temperature at the tantalum L<sub>III</sub> edge, from 9700 to 11 000 eV, with a 2 eV step in the transmission mode. The data analysis was performed by standard procedures using either the suite of programs EXAFSPAK developed by G. George of SSRL or the one developed by A. Michalowicz.<sup>49</sup> Each spectrum was carefully extracted, and the best removal of low-frequency noise was checked by further Fourier transformation. Fitting of the spectrum was done on the *k*<sup>3</sup> weighted data using the following EXAFS equation where *S*<sub>0</sub><sup>2</sup> is the scale factor; *N*<sub>*i*</sub> is the coordination number of shell *i*; *S*<sub>*i*</sub> is the central atom loss factor for atom *i*; *F*<sub>*i*</sub> is the EXAFS scattering function for atom *i*; *R*<sub>*i*</sub> is the distance to atom *i* from the absorbing atom; *λ*<sub>*i*</sub> is the photoelectron mean free path; *σ*<sub>*i*</sub> is the Debye–Waller factor; *φ*<sub>*i*</sub> is the EXAFS phase function for atom *i*; and *φ*<sub>*c*</sub> is the EXAFS phase function for the absorbing atom.

$$\chi(k) \cong S_0^2 \sum_{i=1}^n \frac{N_i S_i(k, R_i) F_i(k, R_i)}{k R_i^2} \exp\left(\frac{-2R_i}{\lambda(k, R_i)}\right) \times \exp(-2\sigma_i^2 k^2) \sin[2kR_i + \phi_i(k, R_i) + \phi_c(k)]$$

The program FEFF<sup>750</sup> was used to calculate theoretical values for *S*<sub>*i*</sub>, *F*<sub>*i*</sub>, *λ*<sub>*i*</sub>, *φ*<sub>*i*</sub>, and *φ*<sub>*c*</sub> based on model clusters of atoms in which atomic positions were taken from the crystal structure of the most similar complexes. The refinements were performed by fitting the structural parameters *N*<sub>*i*</sub>, *R*<sub>*i*</sub> and *σ*<sub>*i*</sub>. The fit residue, *ρ*, was calculated by the following formula:

$$\rho = \frac{\sum_k [k^3 \chi_{\text{exp}}(k) - k^3 \chi_{\text{cal}}(k)]^2}{\sum_k [k^3 \chi_{\text{exp}}(k)]^2}$$

**Reaction of Silica Partially Dehydroxylated at 700 °C with [Ta(CHtBu)(CH<sub>2</sub>tBu)<sub>3</sub>], Formation of the Solid 1.** A mixture of [Ta(CHtBu)(CH<sub>2</sub>tBu)<sub>3</sub>] (0.155 g, 0.33 mmol) in pentane (10 mL) and SiO<sub>2</sub>-(700) (1.0 g) was stirred at 25 °C for 2 h. After filtration, the solid was washed three times with pentane. The solvent was then removed, and the yellow orange solid was dried under dynamic-vacuum at 25 °C.

**Reaction of Silica Partially Dehydroxylated at 700 °C with [Cp\*TaMe<sub>4</sub>]: Formation of the Solid 2.** A mixture of Cp\*TaMe<sub>4</sub> (42.5 mg, 0.11 mmol, 1.2 equiv) and SiO<sub>2</sub>-(700) (373 mg) in pentane (5 mL) was stirred at 25 °C for 2 h. After filtration, the solid was washed three times with pentane and all volatile compounds were condensed into another reactor (of known volume) to quantify methane evolved during the grafting. The resulting yellow powder was dried under vacuum (1.34 Pa) to yield 406 mg of **2**. Analysis by gas chromatography indicated the formation of 86 μmol of methane during the grafting (1.0 nCH<sub>4</sub>/nTa).

**Reactivity of Propane on Solid 2.** In a 352 mL volume reactor were added 67 mg of solid **2** (12.9 μmol of Ta, 3.5%Ta) and propane

(40) Sanner, R. D.; Carter, S. T.; Bruton, W. J., Jr. *J. Organomet. Chem.* **1982**, 240, 157–162.

(41) Oppolzer, W.; Mirza, S. *Helv. Chim. Acta* **1984**, 67, 730–738.

(42) Hediger, S.; Meier, B. H.; Kurur, N. D.; Bodenhausen, G.; Ernst, R. R. *Chem. Phys. Lett.* **1994**, 223, 283–288.

(43) Metz, G.; Wu, X.; Smith, S. O. *J. Magn. Reson., Ser. A* **1994**, 110, 219–227.

(44) Bennett, A. E.; Rienstra, C. M.; Auger, M.; Lakshmi, K. V.; Griffin, R. G. *J. Chem. Phys.* **1995**, 103, 6951–6958.

(45) Marion, D.; Wuethrich, K. *Biochem. Biophys. Res. Commun.* **1983**, 113, 967–974.

(46) Bielecki, A.; Kolbert, A. C.; Levitt, M. H. *Chem. Phys. Lett.* **1989**, 155, 341–346.

(47) Levitt, M. H.; Kolbert, A. C.; Bielecki, A.; Ruben, D. J. *Solid State Nucl. Magn. Reson.* **1993**, 2, 151–163.

(48) Lesage, A.; Duma, L.; Sakellariou, D.; Emsley, L. *J. Am. Chem. Soc.* **2001**, 123, 5747–5752.

(49) Michalowicz, A. *Logiciels pour la chimie*; Société Française de Chimie: Paris, 1991.

(50) Zabinsky, S. I.; Rehr, J. J.; Aukudinov, A.; Albers, R. C.; Eller, M. J. *Phys. Rev. B: Condens. Matter* **1995**, 52, 2995–3009.



(495 Torr, 9.38 mmol). The reaction mixture was heated at 150 °C for 120 h, during which small aliquots were analyzed by GC and GC/MS.

**Reactivity of Propane on Solid 1.** In a 235 mL volume reactor were added 60 mg of solid **1** (12.9  $\mu$ mol Ta, 3.9%<sub>Ta</sub>) and propane (600 Torr, 7.59 mmol). The reaction mixture was heated at 150 °C for 120 h, during which small aliquots were analyzed by GC and GC/MS.

## Conclusion

Generally, whether using  $[\text{Ta}(\text{=CH}t\text{Bu})(\text{CH}_2t\text{Bu})_3]$  or  $[\text{Cp}^*\text{Ta}(\text{CH}_3)_4]$ , the reaction with a silica partially dehydroxylated at 700 °C provides primarily the corresponding monosiloxy surface complexes  $[(\text{=SiO})\text{Ta}(\text{=CH}t\text{Bu})(\text{CH}_2t\text{Bu})_2(\text{=SiOSi=})]$  (**1a'**) and  $[(\text{=SiO})\text{Ta}(\text{CH}_3)_3\text{Cp}^*(\text{=SiOSi=})]$  (**2a'**), by eliminating a  $\sigma$ -bonded ligand as the corresponding alkane ( $\text{H}-\text{CH}_2t\text{Bu}$  or  $\text{H}-\text{CH}_3$ ). Moreover, when the metal is grafted, the coordination number is increased by coordination of a pair of electrons from the siloxane bridge, probably to stabilize the structure. In particular, in the case of  $[\text{Ta}(\text{=CH}t\text{Bu})(\text{CH}_2t\text{Bu})_3]$ , the surface silanol  $[\text{=SiOH}]$  reacts preferentially with the carbene, to yield  $[(\text{=SiO})\text{Ta}(\text{=CH}t\text{Bu})(\text{CH}_2t\text{Bu})_2(\text{=SiOSi=})]$ , which is further stabilized by an additional C–H agostic interaction. In the case of  $[\text{Cp}^*\text{Ta}(\text{CH}_3)_4]$ , the size of the complex is such that after grafting some surface silanols do not become accessible but interact with adjacent  $\text{Cp}^*$  ligands as evidenced by a strong upfield shift of this signal.

In conclusion, the combined evidence presented here shows the possibility for silica partially dehydroxylated at 700 °C to act as a LX ligand in the Green formalism,<sup>3,51,52</sup> rather than an X ligand, as is the most commonly reported. Moreover, the formation of well-defined species characterized at a molecular

level provides the possibility for one to probe mechanisms in heterogeneous catalysis through structure–activity relationship. In particular, in the case of alkane metathesis, the absence of activity of  $[(\text{=SiO})\text{Ta}(\text{CH}_3)_3\text{Cp}^*(\text{=SiOSi=})]$  (**2a'**) and the product selectivity when  $[(\text{=SiO})\text{Ta}(\text{=CH}t\text{Bu})(\text{CH}_2t\text{Bu})_2(\text{=SiOSi=})]$  (**1a'**) was used as a catalyst precursor show that the active site is required to be highly electrophilic, coordinatively unsaturated, and probably involves a metallacyclobutane intermediate. We are currently trying to probe the other steps of the mechanisms such as how the alkane is activated and how the olefins are formed.

This insight was gained by the combined use of several analytical techniques, with particular relevance given to the necessity to complement more traditional spectroscopic data (IR, one-dimensional solid-state NMR...) with data from techniques such as EXAFS and multidimensional NMR spectroscopies.

**Acknowledgment.** M.C. and E.L.R. are grateful to the ministry of education, research & technology, and BP Chemicals for predoctoral fellowships, respectively. We thank M. El Eter for providing helpful data on molecular tantalum complexes. We thank B. M. Maunders for helpful discussions. We also wish to thank Drs. V. Briois and S. Belin for their help in the recording of the EXAFS data on XAS4/D44 at L.U.R.E., Orsay, France (project n° CK 897-02). This work has also been sponsored by BP Chemicals, the CNRS, ENS Lyon, and ESCPE Lyon.

**Supporting Information Available:** NMR spectra. This material is available free of charge via the Internet at <http://pubs.acs.org>.

(51) Elschenbroich, C.; Salzer, A.; Eds. *Organometallics: A Concise Introduction*, Second, Revised Edition; VCH: New York, 1992.

(52) Green, M. L. H. *J. Organomet. Chem.* **1995**, 500, 127–148.